Synthesis of TiO$_2$-doped SiO$_2$ composite films and its applications

XIAOJUN ZHANG[*,†] **and HUAGUI ZHENG**[†]

*Anhui Key Laboratory of Functional Molecular Solids, College of Chemistry and Materials Science, Anhui Normal University, Wuhu 241000, P.R. China

[†]Department of Chemistry, University of Science and Technology of China, Hefei, Anhui 230026, P.R. China

Abstract. The TiO$_2$-doped SiO$_2$ composite films were prepared by two-step sol–gel method and then it was applied in the degradation of methylene red (MR) as photocatalysts. In XRD, FT–IR, and TEM investigations of these TiO$_2$-doped SiO$_2$ composite films, the titanium oxide species are highly dispersed in the SiO$_2$ matrixes and exist in a tetrahedral form. And special attention has been focused on the relationship between the local structure of the titanium oxide species in the TiO$_2$-doped SiO$_2$ composite films and the photocatalytic reactivity in order to provide vital information for the design and application of such highly efficient photocatalytic systems in the degradation of toxic compounds diluted in a liquid phase.

Keywords. Nanostructure; thin films; chemical synthesis; TiO$_2$; SiO$_2$.

1. Introduction

In the last two decades, due to the non-toxic and insoluble nature, titanium oxide catalysts have attracted a great deal of attention as potential photocatalysts to address urgent and global environmental concerns. The photocatalytic degradation of various toxic compounds in aqueous solutions using fine titanium oxide particles has been studied by many researchers (Kudo and Kudo 2006; Tran and Nosaka 2006; Chueh and Hsieh 2007; Ghicov and Schmidt 2007; Hu and Dai 2007; Macak and Zlamal 2007; Meng and Hao 2007; Wang and Ma 2007; Weiher and Beesley 2007; Yu and Yu 2007). However, to avoid the filtration and suspension of small particle photocatalysts, the composite supports containing titania with silica, alumina or other metal oxides have been proposed (Alexeev and Chin 2005; Chu and Inoue 2005; Feng and Miedaner 2005; Yang and Zeng 2005; Li and Wu 2006; Zhang and Zhou 2006). As to catalysts, since the composite binary oxide support combines both the mechanical properties of silica and the chemical properties of active titania, recent studies reveal that TiO$_2$–SiO$_2$ provides the optimal support (Hattori and Shimoda 1999; Panayotov and Paul 2003; Permpoon and Berthome 2006; Lee and Omolade 2007). Recently, silica, titania and silica–titania materials have been obtained by sol–gel method extensively. And the sol–gel process is expected to offer unique advantages for the preparation of such highly dispersed tetrahedrally coordinated and transparent photocatalysts, especially to be applied for coating material, active thin-film photocatalysts, and multicom-ponent ceramics (An and Meng 2006; Liu and Davis 2006; Marugan and Lopez 2006). However, many preparation methods of Ti–Si mixed oxides are through the simultaneous hydrolysis of the metal alkoxides, viz. one-step sol–gel method. And in the hydrolysis process, many Ti–O–Si bands are produced. Therefore, when the as-prepared composite films were additionally annealed, the Ti–O–Si bands ruptured easily for the easiness of TiO$_2$ changing to crystal, which will destroy the structure of the pores.

In the present study, we deal with the preparation of highly active titanium oxide species embedded into transparent SiO$_2$ matrixes using two-step sol–gel method. Special attention has been focused on the relationship between the local structure of the titanium oxide species in the TiO$_2$-doped SiO$_2$ composite films and the photocatalytic reactivity in order to provide vital information for the design and application of such highly efficient photocatalytic systems in the degradation of toxic compounds diluted in a liquid phase.

2. Experimental

The TiO$_2$-doped SiO$_2$ composite films were prepared by a simple method at room temperature and in ambient pressure.

First of all, analytical grade tetraethoxysilane (TEOS, 98%), alcohol, HNO$_3$ and deionized water were mixed together in the molar ratio, 1 : 7 : 1 : 10. The mixture was stirred magnetically till it became a homogeneous solution, which served for dip-coating. The mesoporous silica films were obtained by dip-coating 1 mm thick substrate glasses into the dip-coating solution. The films were dried

---

*Author for correspondence (zhangxj@mail.ustc.edu.cn)

and aged in a sealed box with several pinholes on the top cover under 50°C. The porous SiO_2 films were thus obtained. Secondly, analytical grade tetrabutyl titanate, alcohol and acetic acid (95%) was mixed together in the volume ratio $1:40:5$ (Ti : Si = 1 : 1). The mixture was stirred magnetically till it became a homogeneous solution. And now, several pieces of the pre-formed porous SiO_2 films were, respectively, soaked in the mixture. The films were also dried and aged in a sealed box with several pinholes on the top cover under 50°C. To study the heat effect of our samples, the as-prepared composite films were additionally annealed at 200, 400, 500, 600, 800°C for 10 h.

X-ray diffraction (XRD) measurements were carried out to examine the crystalloid of our samples. The X-ray diffraction (XRD) patterns were collected on Japan Rigaku D-max γA diffractometer with graphite monochromized CuKα radiation ($\gamma = 0.15418$ nm). Transmission electron microscope (TEM) was performed by a Hitachi model H-800 transmission electron microscope with an accelerating voltage of 200 kV. The composition of the products was analysed by X-ray photoelectron spectroscopy (XPS), which was recorded on VGESCALAB MK‖X-ray photoelectron spectrometer using non-monochromatized MgKα ($h\nu = 1253.6$ eV) X-ray as the excitation source. The optical absorption spectra were measured on UV-365. The spectrophotometer recorded was in the range from 250–800 nm at room temperature.

3. Results and discussion

X-ray diffraction profiles of TiO_2-doped SiO_2 composite catalyst films calcined at various temperatures are shown
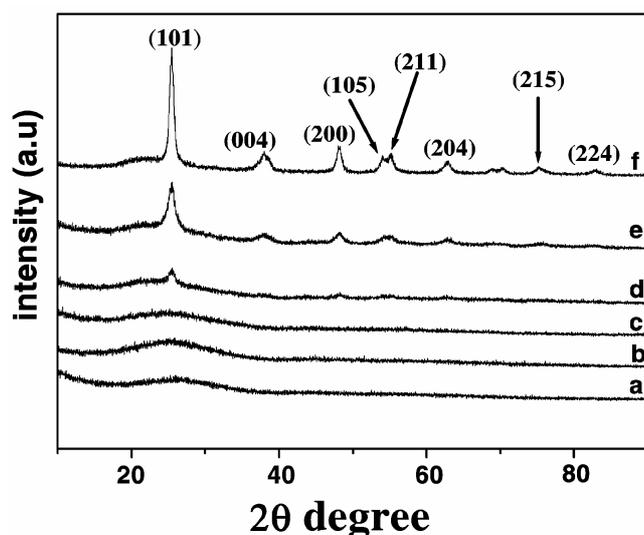
in figure 1. In the pattern, the typical halo peak around $2\theta = 23°$ was attributed to the amorphous SiO_2 matrix, and the diffractogram consists of broad diffraction peaks of TiO_2 anatase (JCPDS file No. 84-1286), with no evidence of the presence of either rutile (JCPDS file No. 78-2485). The anatase peaks are very broad and not well defined, indicating a lack of good crystallinity. However, with increase in calcination temperature there is an increase in the intensity of these peaks indicating an improvement in the crystallinity of the material.

Figure 2 shows the FTIR spectra of TiO_2-doped SiO_2 composite films having different calcined temperatures. With these composite films, five characteristic bands can be observed at around 3300, 1600, 1100, 950, and 650 cm^{-1} (Liu and Davis 1994; Davis and Liu 1997). SiO_2 and TiO_2-doped SiO_2 composite films having a band at around 1100 cm^{-1} can be assigned to the stretching of Si–O–Si bond in the tetrahedral SiO_4 unit of the SiO_2 matrixes. And the band at 3300 and 1600 cm^{-1} are due to O–H bending vibrations of the silinol groups (Nakagawa and Ono 1983; Sohn and Jang 1991). TiO_2 and TiO_2-doped SiO_2 composite films exhibit a band at around 650 cm^{-1} which is representative of TiO_2 matrixes, while the TiO_2-doped SiO_2 composite films exhibit an additional weak band at around 950 cm^{-1}. This band has been assigned to the stretching of the Si–O$^-$ species of Si–O–Ti or Si–O$^-$ defect sites which are formed by the inclusion of Ti^{4+} ions into the SiO_2 matrixes as reported in the previous literature (Davis and Liu 1997). But, compared with other SiO_2–TiO_2 composite, the band observed in our sample at around 950 cm^{-1} is weak (Davis and Liu 1997). We suggest that the tiny titanium dioxide species are embedded into SiO_2 matrixes.

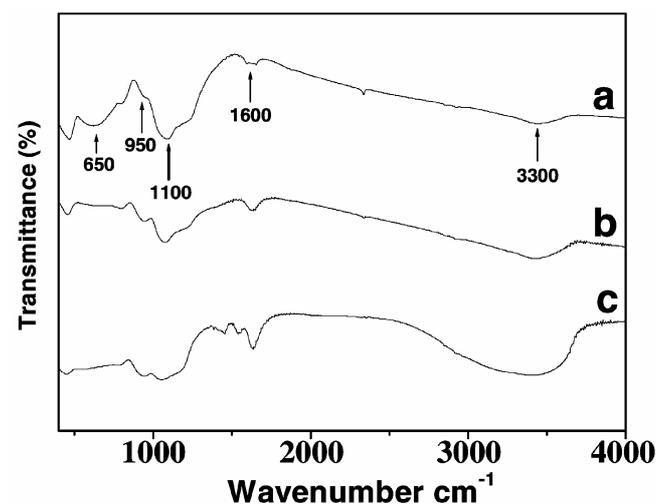Figure 3 shows the TEM micrographs of TiO_2-doped SiO_2 composite films. Images (a), (b) and (c) represent

Figure 1. Powder XRD pattern of the as-synthesized TiO_2-doped SiO_2 composite films **a**. without calcination and calcined at **b**. 200°C, **c**. 400°C, **d**. 500°C, **e**. 600°C and **f**. 800°C.

Figure 2. FT–IR absorption spectra of TiO_2-doped SiO_2 composite films **a**. without calcination, calcined at **b**. 500°C and **c**. 800°C.
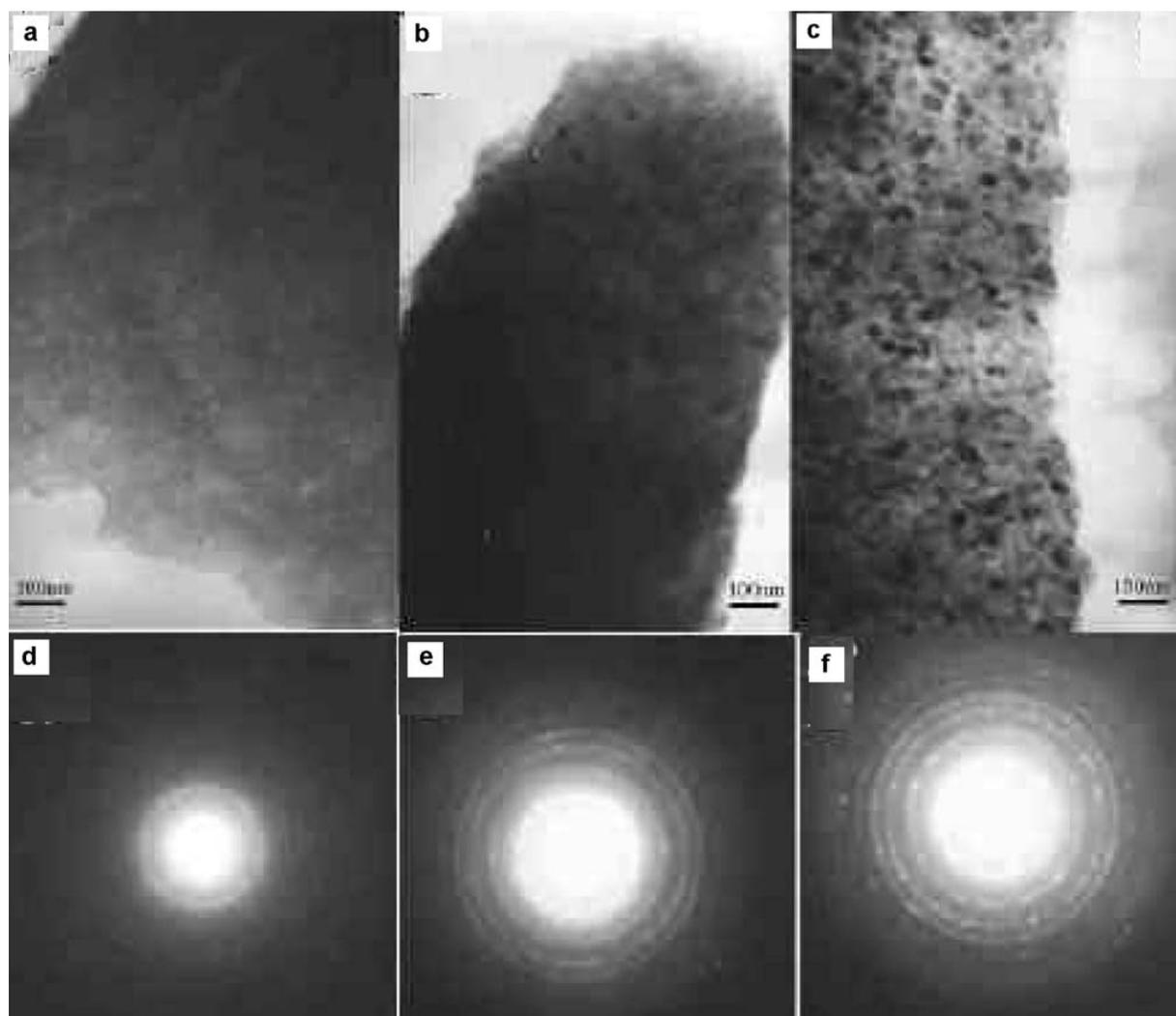
Figure 3. TEM image and selected-area ED pattern of the as-synthesized TiO₂-doped SiO₂ composite films **a**, **d**. without calcinations, **b**, **e**. calcined at 500°C and **c**, **f**. calcined at 800°C.
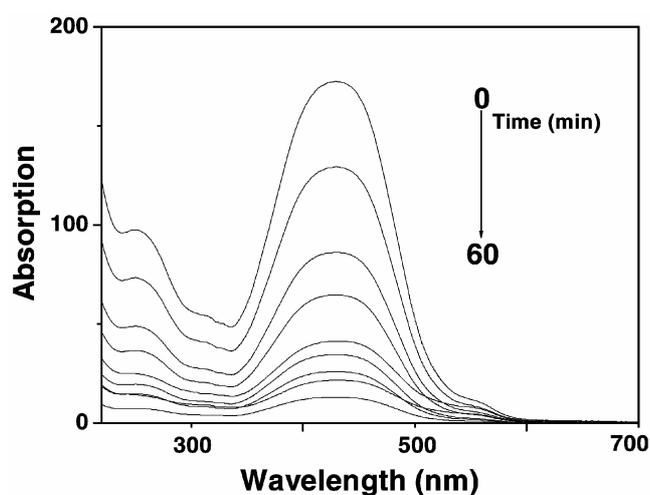

Figure 4. Absorption spectra of a solution of MB (20 ppm) in the presence of 10 mg TiO₂-doped SiO₂ composite films calcined at 500°C under exposure to UV light.

the morphology micrographs of the sample without annealing and annealed at 500 and 800°C for 10 h, showing nearly spherical particles highly uniformly dispersed within the silica glass. The mean particle sizes measured from images (b) and (c) are about 5 and 15 nm, respectively. It suggests that annealing induced the growth of TiO₂ particles dispersed in the glass matrix. The pores in mesoporous SiO₂ matrix are highly dispersive and the possible flow of TiO₂ sol between adjacent pores in the soaked samples during gel progress is somewhat avoided due to the surface tension of the solution, these probably making the TiO₂ particles in our sample less aggregated and well dispersed. From the result of the TEM and ED analysis, we suggested that with increasing annealing temperature, the TiO₂ particles dispersed in the films become bigger, which indicates that the TiO₂ has a relatively high mobility in our films.

To evaluate the photocatalytic activity of the three samples, we have used them to degrade the methylic red
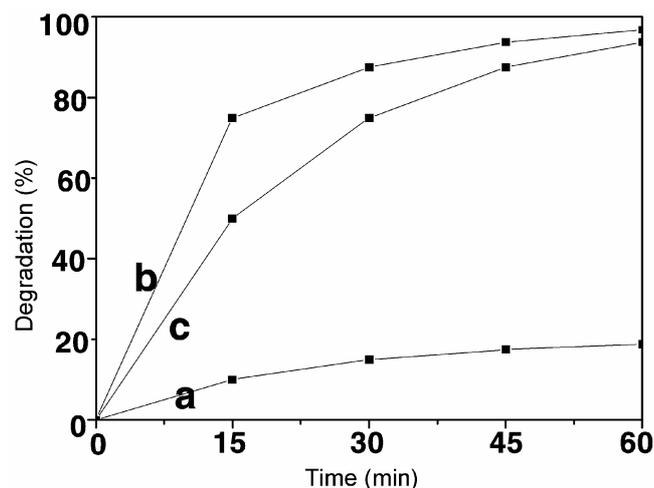
Figure 5. Photocatalytic performances of various samples: TiO_2-doped SiO_2 composite films **a**. without calcination and **b**. calcined at 500°C and **c**. calcined at 800°C.

(MR) in the solution, respectively. In a typical process, 10 mg of TiO_2-doped SiO_2 composite film was added to 100 mL of a MR (20 ppm) solution and magnetically stirred in dark for about 15 min, which allowed it to reach adsorption equilibrium and uniform dispersal. And then the magnetically stirred solution was exposed to UV irradiation from a 250-W high-pressure Hg lamp at room temperature. The samples were collected every 10 min to measure the MR degradation by UV-vis spectra. TiO_2-doped SiO_2 composite films in the collected solution was removed by using centrifugal method. Figure 4 shows the evolution of MR absorption spectra in the presence of 10 mg of TiO_2-doped SiO_2 composite films, from which we can see that the concentration of MR decreased rapidly. In figure 5, we plotted the change in the concentration of MR which was determined according to the characteristic peak at around 400 nm in the UV-vis spectra. It is obvious that TiO_2-doped SiO_2 composite films annealed at 500°C exhibited superior photoactivities over the others, indicating that the appropriate annealing temperature could improve their photoactivities performance. Compared with the photocatalytic activity of three samples, we suggested that the appropriate size of TiO_2 obtained by appropriate annealing temperature will bring out the best result.

4. Conclusions

The TiO_2-doped SiO_2 composite films were prepared by two-step sol–gel method and used as photocatalysts. In XRD, FT–IR, and TEM investigations of these TiO_2-doped SiO_2 composite films, the titanium oxide species are highly dispersed in the SiO_2 matrixes and exist in a tetrahedral form. Detailed analysis of the results prove that TiO_2-doped SiO_2 composite films annealed at 500°C exhibited superior photoactivities over the others, indicating that the appropriate annealing temperature could improve their photoactivities performance.

References

Alexeev O S and Chin S Y 2005 *J. Phys. Chem.* **B109** 23443
An X and Meng G 2006 *J. Phys. Chem.* **B110** 222
Chu S Z and Inoue S 2005 *Langmuir* **21** 8035
Chueh Y L and Hsieh C H 2007 *Adv. Mater.* **19** 143
Davis R J and Liu Z 1997 *Chem. Mater.* **9** 2311
Feng J and Miedaner A 2005 *J. Am. Chem. Soc.* **127** 14968
Ghicov A and Schmidt B 2007 *Chem. Phys. Lett.* **433** 323
Hattori A and Shimoda K 1999 *Langmuir* **15** 5422
Hu L H and Dai S Y 2007 *J. Phys. Chem.* **B111** 358
Kudo T and Kudo Y 2006 *Chem. Lett.* **35** 1390
Lee D and Omolade D 2007 *Chem. Mater.* **19** 1427
Li Y and Wu C Y 2006 *Environ. Sci. Technol.* **40** 6444
Liu Z and Davis R J 1994 *J. Phys. Chem.* **98** 1253
Macak J M and Zlamal M 2007 *Small* **3** 300
Marugan J and Lopez M 2006 *Ind. Eng. Chem. Res.* **45** 8900
Meng S and Hao W C 2007 *Chin. Phys. Lett.* **24** 256
Nakagawa Y and Ono O 1983 *J. Chem. Soc., Faraday Trans.* **79** 2929
Panayotov D A and Paul D K 2003 *J. Phys. Chem.* **B107** 1057110575
Permpoon S and Berthome G 2006 *J. Mater. Sci.* **41** 7650
Sohn J R and Jang H J 1991 *J. Catal.* **132** 563
Tran T H and Nosaka A Y 2006 *J. Phys. Chem.* **B110** 25525
Wang J and Ma T 2007 *Catal. Commun.* **8** 607
Weiher N and Beesley A M 2007 *J. Am. Chem. Soc.* **129** 2240
Yang H G and Zeng H C 2005 *J. Am. Chem. Soc.* **127** 270
Yu H G and Yu J G 2007 *Nanotech.* **18** 065604
Zhang Z and Zhou Y 2006 *Catalysts Energy & Fuels* **20** 2293